Progress in Organic Coatings 216 (2026) 110148

Contents lists available at ScienceDirect

Progress in Organic Coatings

journal homepage: www.elsevier.com/locate/porgcoat

Graphene nanoplatelets (GNPs) as surface-applied protective treatment for paints in outdoor: application to contemporary muralism

Nicolò Guarnieri [a], Sara Goidanich [a,*], Christos Tsakonas [b,d], George Gorgolis [b,d], Maria Giovanna Pastore Carbone [b], George Paterakis [b,d], Gianlorenzo Bussetti [c], Costas Galiotis [b,d], Lucia Toniolo [a]

[a] Department of Chemistry, Materials and Chemical Engineering "Giulio Natta", Politecnico di Milano, Italy
[b] Institute of Chemical Engineering Sciences, Foundation for Research and Technology – Hellas (FORTH/ICE-HT), Patras, Greece
[c] Department of Physics, Politecnico di Milano, Milan, Italy
[d] Department of Chemical Engineering, University of Patras, Patras, Greece

ARTICLE INFO

Keywords:
Graphene Related Materials
2D Materials
Graphene Nanoplatelets
Protective Coatings
Conservation
Street Art
Colour Fading
Photodegradation

ABSTRACT

The preservation of outdoor organic paints constitutes a major challenge due to the rapid degradation of synthetic materials caused by atmospheric agents. This issue is of particular concern for contemporary muralism, which is increasingly recognised as a significant form of urban heritage. This study explores innovative conservation strategies based on the application of graphene nanoplatelets (GNPs) as a protective surface layer for vinyl-acrylic mural paints containing Pigment Red 112. Rather than embedding GNPs in wet paint as done in earlier studies, in this work, two surface-applied strategies were evaluated. A "GNPs layer" approach which consists of applying GNPs onto the dry paint surfaces and aims to provide protection by further exploring the potential to maintain the low material costs and aesthetic alterations, while offering a more versatile solution for existing surfaces. Additionally, a "coated-GNPs layer" approach was developed by overcoating the GNPs layer with a commercial silane-siloxane hydrophobic coating, aimed at enhancing the permanence of GNPs under outdoor exposure. The efficacy of these treatments was evaluated through artificial accelerated ageing (artificial ageing by rain, light, and a combination of both) and characterised using colorimetry, water contact angle measurements, surface roughness analysis, and ATR-FTIR (Attenuated Total Reflectance-Fourier Transform Infrared) spectroscopy. The results demonstrated excellent aesthetic compatibility, with colour changes remaining below the perceptibility threshold (ΔE^*_{ab} <3 CIELAB units) for all application methods. The GNPs layer treatment improved colour stability, increasing the protection factor (percentage reduction in colour change ΔE^*_{ab} of GNPs-treated samples compared to control ones) by 12–26% compared to controls, under light exposure. Furthermore, surface analysis revealed that, in control samples, the contact with the dispersant solution (the liquid medium used to disperse the GNPs and for their application) significant influences the hydrophobicity and roughness of paints. In the coated-GNPs layer, the outer coating exhibited instability under combined ageing. These findings suggest that surface-applied GNPs represent a promising, cost-effective, and minimal-intervention strategy for the conservation and re-treatment of outdoor paints.

1. Introduction

Street art, and particularly its commissioned form known as contemporary muralism, has increasingly been recognised as an important expression of cultural identity and urban heritage in recent years [1]. Over the past two decades, local governments and urban planners have progressively integrated street art into city development strategies, viewing it as a catalyst for cultural vitality and community engagement. Indeed, this artistic form is frequently employed to animate public spaces and to revitalise civic engagement and a sense of belonging among urban populations [2].

However, these artworks often exhibit a dramatically short lifespan, as the materials employed by artists are inherently unstable and rapidly degrade when exposed to outdoor urban environments [3,4].

* Corresponding author.
E-mail address: sara.goidanich@polimi.it (S. Goidanich).

https://doi.org/10.1016/j.porgcoat.2026.110148
Received 29 January 2026; Received in revised form 24 March 2026; Accepted 29 March 2026
Available online 6 April 2026

Contemporary murals are often created using commercial synthetic organic paint formulations (including acrylics, alkyds, styrene-acrylics, and vinyl emulsions, among others), which contain synthetic organic pigments (SOPs), inorganic fillers and various additives to enhance the stability of the paint layers. These materials can be applied in various ways to different surfaces, either directly onto concrete or over simple preparatory plaster layers. While versatile and easy to use, these paints are particularly susceptible to degradation by solar radiation, humidity and meteoric precipitation [3–11].

Colour fading in outdoor murals is rapid and driven mainly by the light-induced photodegradation of pigments and binders [12,13]. Light radiation, both its visible and ultraviolet components, initiates photo-oxidative reactions that generate free radicals within the polymer chains, reacting with oxygen to break chains and reduce molecular weight [12,13]. Photodegradation leads to two major effects: the degradation of organic pigments (SOPs) and the failure of binder cohesion, which in turn results in the detachment and loss of pigment particles from the paint surface [9,12–15]. In addition, binder embrittlement and pigment loss result in a relative enrichment of inorganic fillers at the surface. Studies have shown that colour fading generally affects less than 10 μm of the stratigraphy, while the underlying layers remain largely intact [13,16].

Current protective strategies for outdoor murals rely on commercial coatings adopted from different applications (for example stone conservation) [3]. These materials are typically designed to provide water repellence and UV resistance, but their performance on modern paint systems has often proven inadequate in laboratory and in-situ studies, where they have shown only moderate protection, with low water contact angle values hardly reaching the hydrophobicity threshold and a limited reduction in capillary water absorption [17]. Furthermore, their durability and stability are unsatisfactory, leading to a rapid loss of water repellence and film integrity or adhesion [4,14,18,19]. Moreover, the heterogeneity in commercial paint formulations and execution techniques complicates the effectiveness of standard conservation methods [3,4].

Overall, the lack of long-lasting, aesthetically compatible solutions highlights the need for innovative approaches specifically tailored for the preservation of contemporary murals. Any new solution must be compatible with the substrate, preserve visual appearance, and provide resistance to degradation [4].

Recent advances in graphene-based strategies offer new opportunities for conservation [18,20,21]. The unique properties of graphene, such as high UV absorption, radical scavenging activity, impermeability to gases and liquids, and antimicrobial effects, enable a multifactorial mechanism of action for mitigating photo-oxidative degradation [18,20,22–29]. Several mechanisms contribute to the photo-stabilising effect of graphene, including UV absorption and screening (it has been reported that only ≈30% of radiation in the UV region is transmitted by a single-layer of graphene [18]), radical scavenging activity linked to sp^2 hybridised carbons, quenching ability as an electron acceptor, and physical barrier properties (creating tortuous pathways that hinder the diffusion of oxygen and free radicals) [22]. The combined contribution of these mechanisms has been crucial for achieving optimal photo-stabilisation in some polymeric matrices (polyurethane [27,28], polypropylene [26], chitosan and polyethylene glycol [24]).

Large-area CVD (Chemical Vapour Deposition) graphene films have been employed as protective veils for dye-based artworks on glossy paper, cardboard or canvas substrates, exploiting their excellent barrier properties against UV radiation, oxygen, and moisture [21,30]. Graphene films have been also applied on inkjet-printed photographic paper evaluating their anti-fading action by monitoring the degradation of a common blue dye (crystal violet) [31]. These studies showed the possibility of applying multi-layer graphene coatings to achieve higher protection factors for dyes, reaching values of up to 70% [21]. Nevertheless, the approach raised concerns regarding aesthetic compatibility when multiple layers are applied [21]. While a single graphene layer is nearly transparent (absorbing only 2.3% of visible light), the cumulative absorption of multi-layer configurations can lead to perceptible surface darkening. Furthermore, limitations remain regarding the application on rougher substrates [21].

Unfortunately, this strategy could be hardly implemented for contemporary muralism, due to the large surface area of the murals and the heterogeneity of the substrate. Acar et al. [32] demonstrated that epoxy-based coatings incorporating graphene nanoplatelets (GNPs) applied superficially on wood-plastic composite substrates significantly improved outdoor performance, reducing colour fading and mechanical degradation under accelerated weathering conditions. Furthermore, a study by Kotsidi et al. [20] demonstrated that incorporating liquid-phase exfoliated GNPs into paints and inks, subsequently applied to plaster or cardboard, respectively, can help mitigate colour fading. These materials were shown to enhance the mechanical integrity of paint layers, reduce photodegradation, and improve electrical conductivity, contributing to anti-static effects [20]. The successful formulation of aqueous dispersions of GNPs enables their direct integration into waterborne paint systems, such as those commonly employed in street art murals, ensuring compatibility with existing artistic materials and facilitating scalable application without compromising current artistic practices. In addition, from a cost perspective, GNPs are more economical to produce than graphene veils, carbon nanofibers, or carbon nanotubes [24,33,34].

However, although GNPs have demonstrated potential in mitigating colour fading when incorporated into paint formulations, it is fundamental to ensure the aesthetic compatibility of these additives to prevent any alteration to the original colour of the paints used by artists. Indeed, when GNPs are incorporated in bulk within the paint, achieving the optimal protective effect may lead to undesirable darkening of the materials [27,35]. Furthermore, previous investigations on real murals and accelerated ageing consistently demonstrated that colour fading is predominantly a superficial phenomenon, affecting only the outer microns of the paint layer.

These observations highlight a significant research gap: rather than modifying the entire paint formulation, an unexplored strategy would be to apply GNPs solely to paint surface. This approach could provide a thin protective layer that minimizes visual impact, placing GNPs only where they are needed to act against colour fading [12,13]. This strategy may offer several advantages. Primarily, it requires a reduced quantity of material, which has two important consequences: lowering costs and minimizing the impact on aesthetic compatibility compared to incorporating black powder into coloured paints. Furthermore, it can be applied to existing street artworks, making it highly suitable for conservation interventions and re-treatments.

To validate this concept, this study aims to explore the protective action of GNPs applied onto paint surfaces through a water-based dispersion, based on established protocols from previous works [20]. In particular, a commercial acrylic-vinyl paint containing Pigment Red 112 (PR112, Naphthol AS) was selected, as it had been previously identified as highly vulnerable in real case studies and accelerated ageing tests [11–13], thus making it an ideal model system for testing innovative protective strategies.

Two surface-applied strategies were developed to enhance the protection of mural paints against environmental degradation (Fig. 1). The first approach (Fig. 1a), referred to as “GNPs layer”, involves the application of GNPs onto the surface of fully dried paint layers, similar to certain protective strategies with nanoparticles applied directly to the surface, in the field of stone conservation [36,37]. Three different application methods of GNPs were tested: drop-casting, dipping and spraying. The second approach (Fig. 1b), named as “coated-GNPs layer”, introduces an additional protective/sealant layer on top of the GNPs layer, using a commercial silane-siloxane coating. This configuration was hypothesized to prevent the possible detachment of GNPs from the paint and to enhance surface water repellence. The silane-based layer is intended to improve the adhesion of the GNPs and the long term

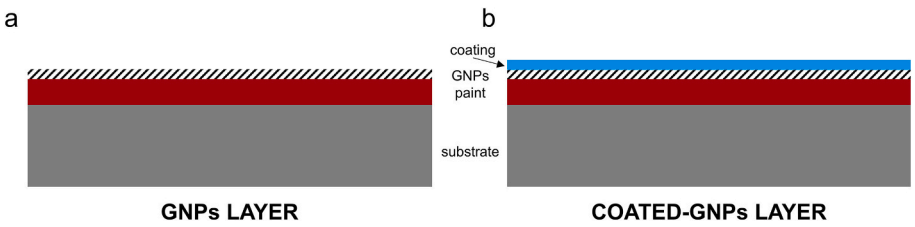

Fig. 1. Schematic representation of the two protective approaches: (a) GNPs layer and (b) coated-GNPs layer. The term "GNP layer" refers to the application of nanoplatelets onto the dry paint, while "coated-GNPs layer" identifies the system of GNPs layer + hydrophobic coating. Both represent the surface-applied treatments proposed for the conservation of existing contemporary mural surfaces.

durability of the treatment, creating a sacrificial barrier against rain and other atmospheric agents; furthermore, this coating matrix ensures that no release of GNPs into the environment can occur, possibly mitigating concerns regarding airborne nanoparticles [38]. Both approaches were conceived for application as a finishing layer or as a protection layer of existing artworks, offering the advantage of minimal intervention and compatibility with conservation practices.

Protective potential of surface-applied treatments was evaluated on paint specimens of commercial waterborne vinyl-acrylic paint containing PR112. The performance and stability of the GNPs layer and coated-GNPs layer proposed treatments were assessed through a comprehensive characterization protocol under accelerated ageing tests protocols reported in previous studies [12]. The analysis combined spectroscopic and imaging techniques, including reflectance VIS-spectroscopy, ATR-FTIR spectroscopy, water contact angle (WCA) measurements, and atomic force microscopy (AFM). This approach allowed for the monitoring of colour alteration, surface morphology, and chemical changes to evaluate the protective efficacy of the proposed strategies.

2. Materials

2.1. Dispersion formation

To obtain a stable aqueous dispersion of graphene nanoplatelets (GNPs), a liquid-phase exfoliation (LPE) method was employed following previously reported protocols [20]. First, 400 mg of graphene nano-powder (Elicarb Electrical grade, Thomas Swan & Co Ltd), were initially pre-exfoliated using a mortar and pestle with a few drops of a binary water/ethanol mixture (ethanol molar fraction 0.06). The powder was then fully dispersed in the same solution system to achieve a final concentration of 2 mg/mL. The solution was subjected to shear mixing at 5000 rpm for 20 min, followed by bath sonication for 3 h. To remove unexfoliated bulk material, the dispersion was centrifuged twice: first for 10 min at 1000 rpm and then for 5 min at 5000 rpm. The resulting supernatant, containing well-dispersed graphene flakes, was collected for subsequent use as the final dispersion (GNP2). A similar dispersion (GNP4) was also prepared by same methodology, adding GNPs to the solution to obtain a concentration of 4 mg/mL.

2.2. Preparation of paint specimens GNPs layer and coated-GNPs layer

Paint specimens were produced by applying a commercial waterborne vinyl-acrylic paint (Red VIP 08, J Colours S.p.A., Italy), pigmented with PR112, onto microscopy glass slides using the blade technique (supplementary fig. 1). These binder-pigment-fillers formulation had previously been assessed as highly prone to colour fading in the literature [10–14].

The first conservation strategy investigated in this study focuses on the application of GNPs as protective coatings on already dried paint layers, simulating real-world scenarios where murals have already been completed, named GNPs layer (Fig. 1a). Three application techniques were initially explored to simulate practical conservation scenarios: (i) *Drop-casting* (DROP), involving direct deposition of aqueous dispersions onto the dried paint surface, followed by manual spreading and ambient drying; (ii) *Dipping* (DIP), consisting of immersing painted glass-slide samples into stirred GNPs dispersions for 1 h to promote passive adsorption and surface deposition; and (iii) *Spraying* (SPRAY), using a manual sprayer to apply aqueous dispersions in three successive passes to ensure uniform coverage. The dipping method was subsequently adopted to prepare the full set of specimens with GNPs layer and coated-GNPs layer treatments, by immersing half of the glass slide in the GNPs dispersion, and the other half in a dispersant solution only, without GNPs (control). The coated samples (Fig. 1b) were obtained by applying, after 3 days of drying, a commercial silane- and siloxane-based protective coating to improve the stability of the GNPs under simulated rainfall and moisture exposure. The coating (SILRES® BS 290, Wacker Chemie AG, supplied by IMCD Italia SpA, Milan, Italy) was diluted at a 1:12 pbw ratio in 2-propanol, as specified in the technical datasheet, and applied both on the GNPs layer and control, to obtain the coated-GNPs layer and coated-control samples. The list of the samples, treatments and their labels is reported in Table 1. "Untreated paint" indicates the bare paint reference as supplied. The two surface-applied treatment configurations are labelled as "GNPs layer" and "coated-GNPs layer" treatments. Both of them have their correspondent control, treated solely with the dispersant solution without GNPs, labelled as "control" and "coated-control".

3. Methods

3.1. Ageing procedure

Samples were subjected to three ageing conditions: rain-only (R), light-only (L) and combined rain followed by light (RL) to evaluate both the individual and the synergistic effects of these environmental stressors on treated surfaces. Table 1 provides a schematic overview of the ageing protocols applied to each sample.

Artificial rain ageing was performed in a custom-built rain chamber (described in detailed in [19]) designed to deliver highly uniform and reproducible rain conditions. The accelerated rain cycle simulated approximately 2 years of cumulative rainfall in Central-Southern Europe [19,39,40]. The protocol consisted of three consecutive days of rain exposure, with a total precipitation of 1440 mm, achieved through cycles of 6 h of heavy rain (83 ± 7 mm/h) followed by 18 h of drying. The rainwater used was demineralized (pH = 6.2, conductivity 1.45 µS/cm) [19,41]. A detailed description of the ageing parameters is reported in [19].

Accelerated light ageing was performed inside a custom-designed light chamber, previously described in [12], equipped with seven spiral compact fluorescent lamps (Walimex pro, 125 W, 5500 K, 5600 lm). The system provided uniform visible illumination with a total light intensity of 50 ± 11 klux.

Specimens were placed horizontally and exposed for 100 days (24/7) under high relative humidity (RH 80.5 ± 11.5%), maintained by a saturated KNO_3 solution. A detailed description and the rationale behind the ageing parameters are reported in [12]. The combined ageing consisted of three days of the artificial rain exposure followed by 100 days of

Table 1
Summary of samples categorized by material, class of treatment, and ageing conditions and respective labels. The samples include untreated paint references, GNPs layer treatments and its respective control (paint treated with dispersant only), coated-GNPs layer treatments and its respective coated-control (commercial coating silane/siloxane), and paint+coating samples.

Class	Name	Material and treatment	Ageing	Label
Untreated paint	Untreated Paint unaged	Untreated paint	Unaged	P-U
	Untreated Paint R		Rain	P-R
	Untreated Paint L		Light	P-L
	Untreated Paint RL		Rain + Light	P-RL
GNPs layer	GNPs layer unaged	Paint + GNPs dispersion	Unaged	GNP-U
	GNPs layer R		Rain	GNP-R
	GNPs layer L		Light	GNP-L
	GNPs layer RL		Rain + Light	GNP-RL
Control	Control unaged	Paint + dispersant only	Unaged	CTRL-U
	Control R		Rain	CTRL-R
	Control L		Light	CTRL-L
	Control RL		Rain + Light	CTRL-RL
Coated-GNPs layer	Coated-GNPs layer unaged	Paint + GNPs dispersion + coating	Unaged	C-GNP-U
	Coated-GNPs layer R		Rain	C-GNP-R
	Coated-GNPs layer L		Light	C-GNP-L
	Coated-GNPs layer RL		Rain + Light	C-GNP-RL
Coated-control	Coated-control unaged	Paint + dispersant only + coating	Unaged	C-CTRL-U
	Coated-control R		Rain	C-CTRL-R
	Coated-control L		Light	C-CTRL-L
	Coated-control RL		Rain + Light	C-CTRL-RL
Coating	Coating unaged	Paint + coating	Unaged	C-U
	Coating R		Rain	C-R
	Coating RL		Rain + Light	C-RL

accelerated light ageing. This protocol aimed to evaluate whether the mechanical action of raindrops could remove the applied GNPs and to assess their protective effect against colour fading.

3.2. Characterization methods

Colour fading after the ageing process was assessed through VIS reflectance spectroscopy (Spectro-colourimeter CM-2600d, Konica Minolta, Tokyo, Japan), employing a D65 light source at 10° and an 8 mm spot size. For each painted specimen, 10 measurements were recorded. The data were processed in the CIELAB colour space. L* represents lightness, a* and b* represent the red-green and yellow-blue axis, respectively. Additionally, the chroma (C^*_{ab}), indicating the saturation or intensity of the colour, was calculated according to formula (1). To quantify the total perceived colour difference between states, ΔE^*_{ab} values were determined according to the formula (2) [42,43]. According to [44], a total colour difference of 3.5 CIELAB units was adopted as the maximum threshold of tolerability for aesthetic compatibility. To compare the colorimetric coordinates after ageing of control samples ($\Delta E^*_{ab}control$) with those of treated with GNPs ($\Delta E^*_{ab}GNPs$), a protection factor (PF) was determined according to the formula (3) [20]. This parameter allows to estimate the increase of colour stability of the addition of the GNPs respect to the control samples treated only with the dispersant solution without GNPs. Results are expressed as the mean value ± standard deviation in the figures.

$$C^*_{ab} = \sqrt{a^{*2} + b^{*2}} \tag{1}$$

$$\Delta E^*_{ab} = \sqrt{(\Delta L^*)^2 + (\Delta a^*)^2 + (\Delta b^*)^2} \tag{2}$$

$$PF(\%) = \frac{\Delta E^*_{ab}control - \Delta E^*_{ab}GNPs}{\Delta E^*_{ab}control} \tag{3}$$

Surface morphology was examined by optical microscopy (Leica DM6 3D, Leica Microsystems, Milan, Italy), using objectives between 20× and 50× and the LASX software version 5.1.0.25593. To estimate surface roughness, two 3D reconstructed images were acquired for each sample using a 50× objective. From each image, 25 surface profiles were extracted (with lengths ranging between 0.12 and 0.20 mm), resulting in a total of 50 profiles per sample. The roughness parameter R_q (root mean square roughness, defined as the square root of the mean square of the profile height deviations from the mean line) was calculated for each profile and then averaged to obtain a representative value for the sample. Data were averaged and are presented as mean values ± standard deviation.

The wetting properties of pristine and treated paints were evaluated by static water contact angle (WCA) measurements using a Krüss Easydrop instrument equipped with Drop Shape Analysis (DSA) software. For each sample, 15 measurements were performed using Milli-Q water as the test liquid. A 5 μL droplet was deposited on the surface, and the contact angle was recorded 10 s after deposition [17,45]. Averages, standard deviations and statistical tests (student's *t*-test) were computed using Microsoft Excel.

An atomic force microscopy (AFM, Keysigth 5500) was employed to evaluate the surface roughness at the nano length scale of untreated paint, layer GNPs, and control specimens. Equivalent samples were prepared on ultra-flat glass slides (Ossila) and treated following the same protocol adopted for the main experimental specimens, ensuring consistency in application and drying conditions. Prior to AFM analysis, water contact angle (WCA) values were verified to match those measured on the corresponding samples used in the experimentation, confirming equivalence in surface properties.

Surface profiles were acquired by driving AFM in tapping mode over areas of (2×2 μm^2) and data were analysed with a dedicated analysis software (Gwyddion open software). For each sample, different profiles were collected, and representative profiles were extracted for roughness evaluation. The profiles were processed to highlight vertical excursions and surface features, enabling qualitative comparison among untreated paint, GNPs layer, and control.

ATR-FTIR (Attenuated Total Reflectance-Fourier Transform Infrared) spectroscopy (Thermo Nicolet iZ10, equipped with a SmartX accessory, ThermoFisher Scientific Inc., Waltham, MA, USA) was employed to investigate molecular modifications occurring in the specimens after ageing. Spectra were collected with 32 scans at a resolution of 4 cm^{-1}, both before and after the artificial exposure. Compositional variations were assessed by calculating intensity ratios of selected absorption bands, using the "N" method in OPUS software (Bruker Optik GmbH, Ettlingen, Germany, version 8.5), where peak heights were measured relative to their baselines. The following

characteristic vibrations of the paint components were taken into account to evaluate ratio changes due to the treatment and ageing protocols: calcite out-of-plane bending of the carbonate ion (875 cm^{-1}) [6], Outer OH stretching of Al^{VI}-OH (3690 cm^{-1}) [46], the carbonyl group of the binder (1740 cm^{-1}) [47,48], and naphthol pigments (750 cm^{-1}) [49–51]. Averages, standard deviations and statistical tests (student's *t*-test) were computed using Microsoft Excel.

4. Results and discussion

4.1. Evaluation of application methods and aesthetic compatibility of GNPs treatments

Two dispersions of GNPs, with initial concentrations of 2 mg/mL (GNP2) and 4 mg/mL (GNP4), were evaluated to assess the aesthetic compatibility of treatments on painted surfaces. Three different application methods were tested to explore their feasibility and performance. All methods demonstrated excellent aesthetic compatibility, with ΔE^*_{ab} values below 3 CIELAB units (Fig. 2) [44]. Interestingly, the dispersion with the higher concentration (GNP4) resulted in lower colour variations compared to GNP2. However, it must be noted that it was not possible to quantitatively measure the exact quantity of GNPs applied or the degree of surface coverage; this lack of precise quantification may explain such counter-intuitive values, as the actual deposition efficiency might not correlate linearly with concentration.

Regarding the application techniques, the drop-casting method generally resulted in slightly higher ΔE^*_{ab} values than the other two methods. Dipping and spraying applications showed more contained variations, likely due to the smaller amount of material deposited in these cases. Although quantification was not possible, the presence of GNPs was clearly observable through optical microscopy. Optical microscopy observations, in fact, revealed the presence of macro-clusters of GNPs on the paint surfaces for all the observed cases (Fig. 3). Based on these preliminary results, the GNP2 DIP application was selected for subsequent experiments involving GNPs layer and coated-GNPs layer treatments, as well as artificial ageing tests. The choice of DIP application was driven by the ease and reproducibility of the sample preparation process.

4.2. Protective efficacy of GNPs layer and coated-GNPs layer

4.2.1. Colorimetric monitoring

The untreated paint (Fig. 4) confirmed high susceptibility to colour fading when exposed to light, with ΔE^*_{ab} values exceeding 11 CIELAB units, corresponding to very marked differences of perceived colours [44]. When rain ageing preceded light exposure, the final colour change was lower, with ΔE^*_{ab} limited to approximately 4 CIELAB units, indicating that the surface previously modified by rain responds differently to the subsequent light exposure, but still exceeding the threshold of perceptibility (3.5 CIELAB units). Fig. 4 illustrates the untreated unaged paint sample and the minimal colour variation caused by rain ageing alone ($\Delta E^*_{ab} \approx 1$ CIELAB unit), while samples not exposed to light (R and unaged) showed no noticeable chromatic alteration (ΔE^*_{ab} values below 1 CIELAB unit).

For GNPs layer, samples treated with GNPs showed a lower colour change under light ageing compared to the untreated paint (Fig. 5). While a comparison with the untreated paint would yield an *apparent* protection factor (PF) of 60%, this value includes all effects associated with the aqueous treatment itself of the dispersant solution. Indeed, the control (treated with the dispersant solution only) exhibited also a markedly reduced colour change after light ageing (black dashed line in Fig. 5). This indicates that the interaction with the dispersant solution alters the surface in a way that affects the subsequent colour evolution under light, independently of the presence of GNPs. This behaviour can be plausibly linked to the interaction with the polar aqueous environment during treatment, which may induce surface reorganization phenomena or the loss of hydrophilic additives (as calcite). The removal of calcite is particularly relevant, as its surface accumulation is a primary driver of the colour fading mechanism in these paints [12]. For this reason, the PF calculated relative to the untreated paint does not isolate the contribution of the nanoplatelets. The only PF value that can be unambiguously attributed to the presence of GNPs is therefore the difference between the GNPs layer samples and their corresponding control, which amounts to approximately 12% (solid versus dashed lines in Fig. 5). Despite the apparent small magnitude of this net protection, the difference remains statistically significant, as evidenced by error bars in figure, confirming that the GNPs provide a distinct and measurable shielding effect.

When rain exposure preceded light ageing, the difference in PF between the layer GNPs samples and their corresponding layer control increased to approximately 26% (purple lines in Fig. 5). This higher PF reflects the altered surface state induced by rain, which modifies the subsequent colour evolution under light, which accentuates the divergence between the behaviour of the GNPs layer and control.

In coated-GNPs layer systems, applying GNPs prior to the silane-

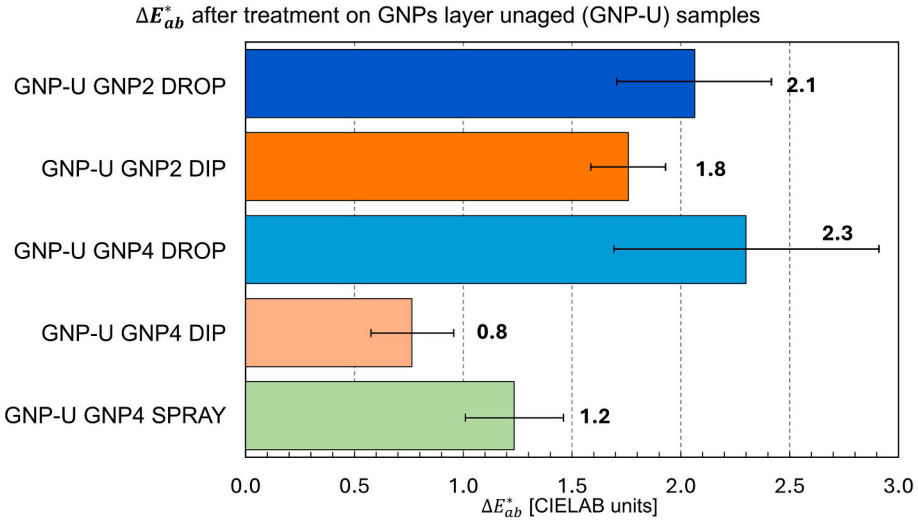

Fig. 2. ΔE^*_{ab} values of GNPs layer samples before and after the application of the GNPs for the different methods (DIP: dipping, DROP: drop-casting, SPRAY: spraying) and concentrations (GNP2 and GNP4).

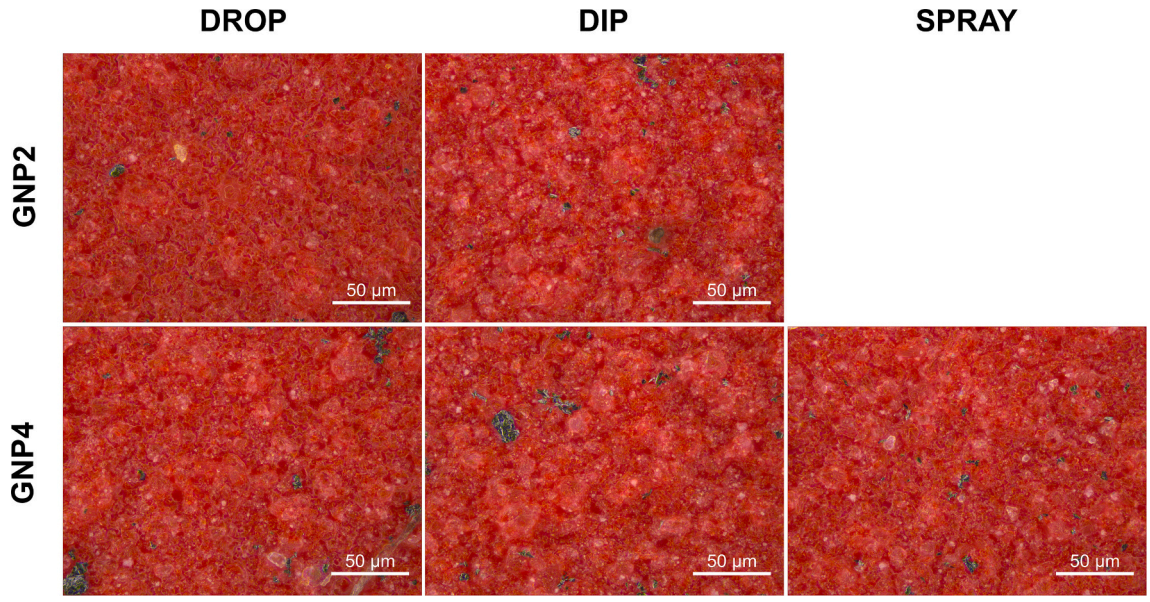

Fig. 3. Optical microscopy images (50×) showing the presence of the GNPs on the surface of the paint of GNPs layer samples.

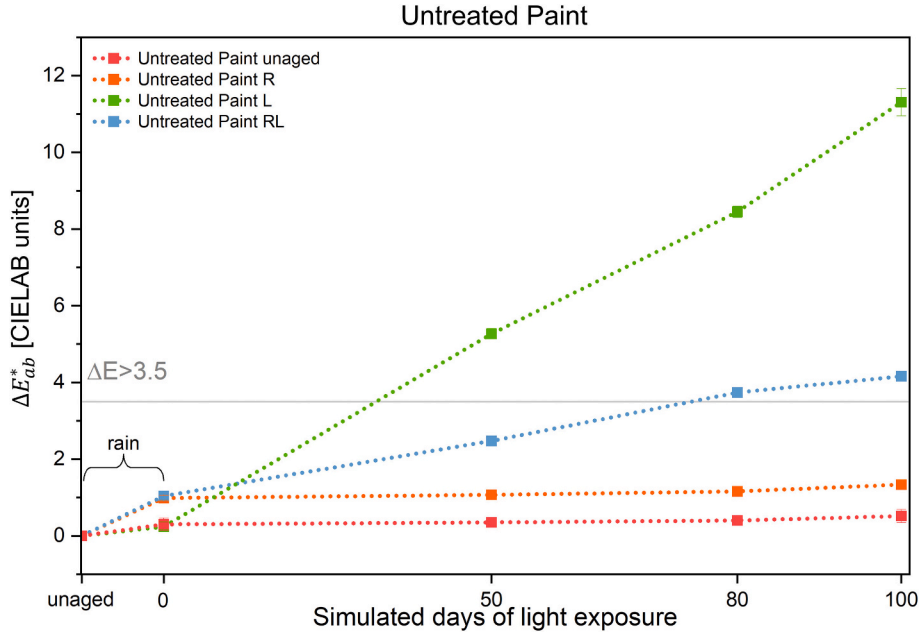

Fig. 4. ΔE^*_{ab} values during rain and light ageing of untreated paint. The grey horizontal line at 3.5 CIELAB units represents the threshold for a "clearly distinct" colour difference perceptible to the human eye, according to [44]. Values below this threshold indicate no perceptible changes after ageing.

siloxane coating led to improved resistance to colour fading compared to respective coated-control treated only with dispersant solution and coated with the silane-siloxane product (brown and olive lines in Fig. 6). The addition of GNPs increased PF with respect to the control, by about 19% (solid lines vs. dashed lines in Fig. 6) in the case of only light ageing alone (brown lines), and 4% for the combined rain and light ageing (olive green lines). Interestingly, combined rain and light ageing produced a more pronounced colour change in coated-GNPs layer samples than light exposure alone, unlike the trend observed for layer treatments and untreated paint (brown lines vs olive green lines in Fig. 6). A plausible explanation is the potential instability of the coating under the combined rain and light exposure, as suggested by the detail shown in Fig. 6, where the coating alone shows higher ΔE^*_{ab} values than coated-GNPs layer samples after rain exposure.

Fig. 7 illustrates the evolution of lightness (L^*) and chroma (C^*_{ab}) coordinates for each sample under the different ageing conditions. Following light ageing, all samples exhibited a trend towards higher L^* and lower C^*_{ab} values, indicating a general brightening and loss of saturation. In contrast, rain ageing alone (R) tended to preserve the chroma coordinate (C^*_{ab}); in some cases, such as the untreated paint, it even resulted in an increase (Fig. 7a). As discussed later, this can be associated to the selective dissolution of white fillers such as $CaCO_3$. Light ageing alone (L) consistently produced the most marked chromatic alterations, characterised by the lowest C^*_{ab} and highest L^* values, particularly for the untreated paint and the layer GNPs treatment. As previously observed, for the coated-GNPs layer (Fig. 7c), combined rain and light ageing (RL) led to the lowest values, suggesting that the additional coating may be more susceptible to degradation under the

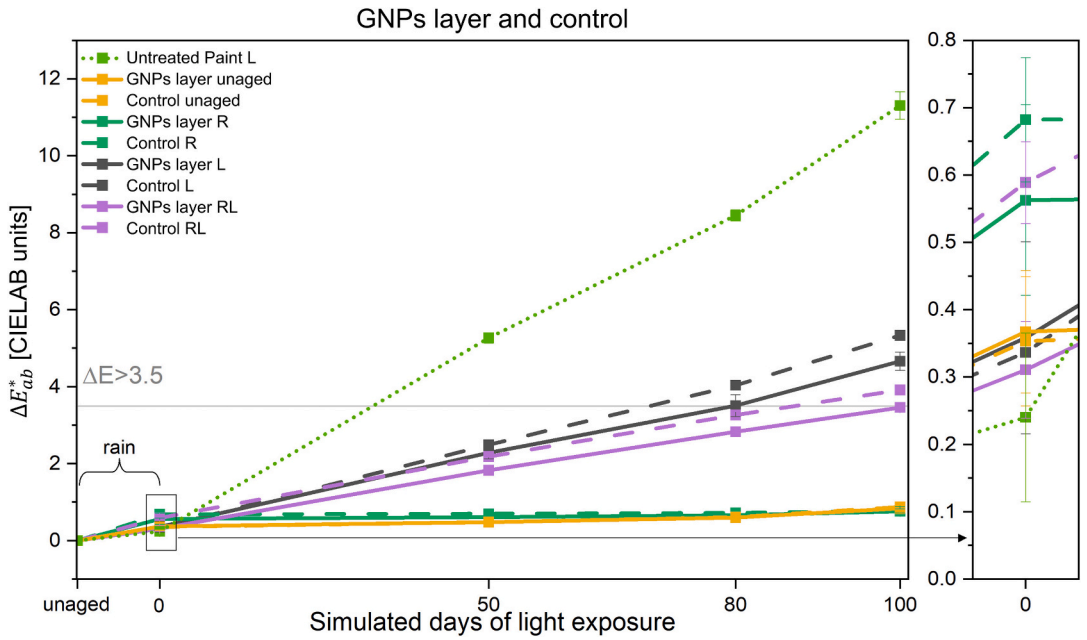

Fig. 5. ΔE^*_{ab} values during rain and light ageing of GNPs layer and respective control. On the right detail of ΔE^*_{ab} due to rain ageing. The grey horizontal line at 3.5 CIELAB units represents the threshold for a "clearly distinct" colour difference perceptible to the human eye, according to [44]. Values below this threshold indicate no perceptible changes after ageing.

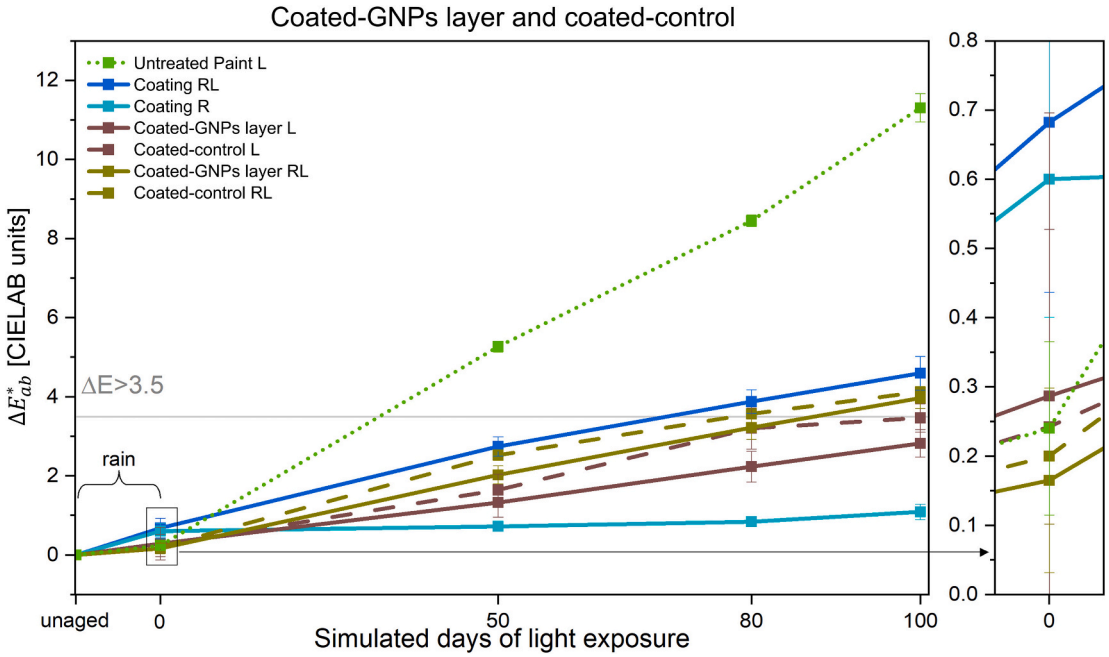

Fig. 6. ΔE^*_{ab} values during rain and light ageing of coated-GNPs layer and respective coated-control. On the right detail of ΔE^*_{ab} due to rain ageing. The grey horizontal line at 3.5 CIELAB units represents the threshold for a "clearly distinct" colour difference perceptible to the human eye, according to [44]. Values below this threshold indicate no perceptible changes after ageing.

synergistic effects of rain and light.

4.2.2. Static contact angles measurements

Untreated unaged paint exhibited low water contact angle (WCA) values, averaging around 70°, with high variability among measurements (Fig. 8a). These results are consistent with typical acrylic-based paints, which generally display hydrophilic behaviour [17,19,52]. Hydrophilic behaviour has been also associated in literature with the presence of mineral fillers such as calcite and kaolin [53–55] and surfactants [56,57]. Acrylic and vinyl-acrylic paints typically contain non-ionic poly(ethylene oxide) (PEO) surfactants, anionic surfactants, protective colloids such as poly(vinyl alcohol) and other water-soluble additives, which form hydrophilic domains [56–62].

Unexpectedly, the GNPs layer treatment produced significantly higher WCA values, approximately 120°, indicating a marked increase in surface hydrophobicity. Interestingly, similar high WCA values were also observed in the control samples, treated only with the dispersant solution without GNPs (Fig. 8b). This suggests that the dispersant

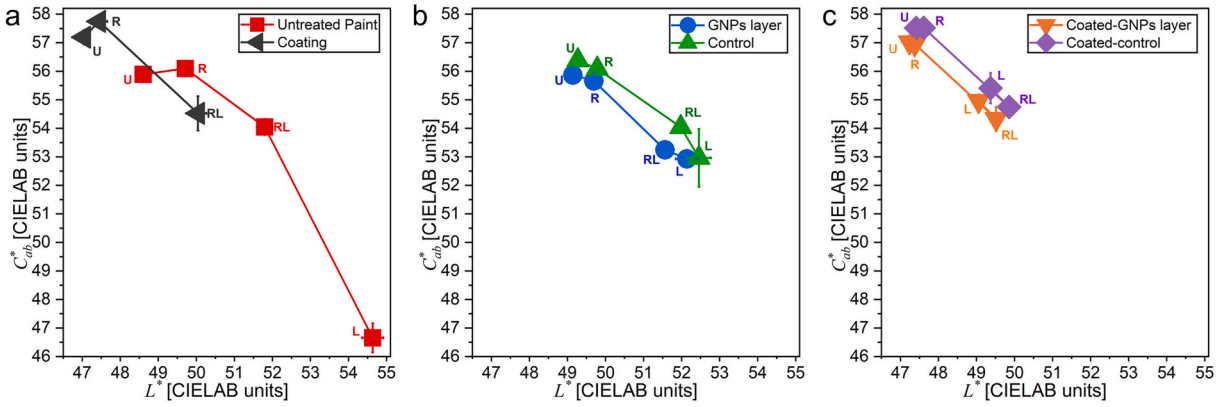

Fig. 7. $L^*C^*_{ab}$ scatter plots of (a) untreated paint (red squares) and coating only (black triangles), (b) GNPs layer (blue circles) and control (green triangles), and (c) coated-GNPs layer (orange triangles) and coated-control (purple diamonds). The different ageing conditions are indicated with labels: U – unaged, R – rain, L – light, RL – combined rain and light. Error bars represent standard deviations.

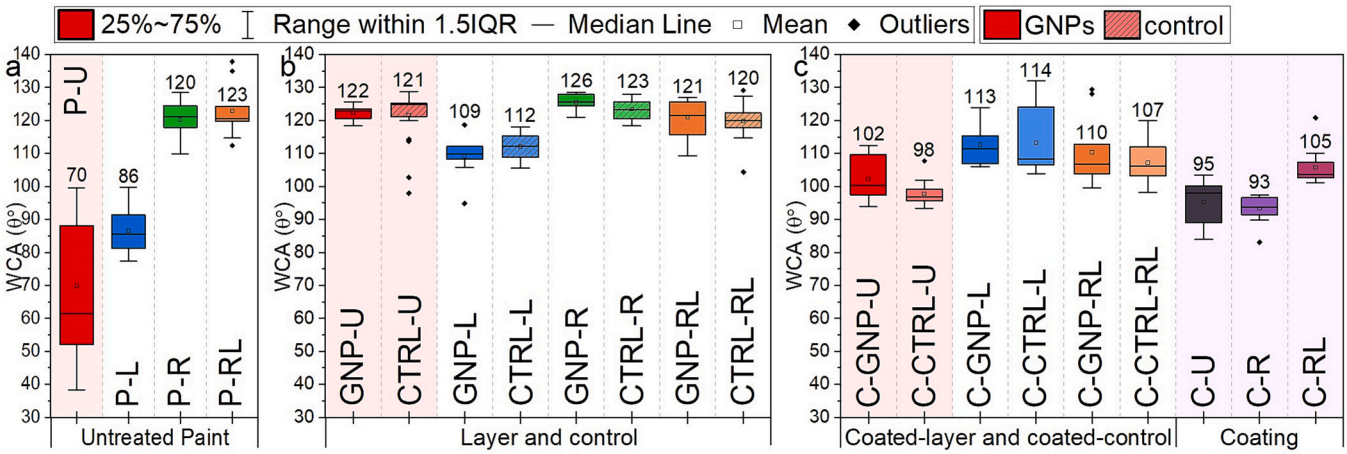

Fig. 8. Water contact angle (WCA) values for (a) untreated paint, (b) GNPs layer treatments, and (c) coated-GNPs layer treatments and coating only. For each category, GNPs-treated samples (solid boxes) and their respective controls (dashed) are shown before (unaged - red) and after artificial ageing (light - blue, rain - green, and combined - orange). Data are presented as box plots to illustrate mean values and variability. (For interpretation of the references to colour in this figure legend, the reader is referred to the web version of this article.)

solution system itself plays a role in modifying surface wettability, while the presence of GNPs does not further enhance hydrophobicity in the layer configuration ($p = 0.70$).

The increase in water contact angle after contact with the aqueous dispersion by dipping, indicates that the paint surface becomes more hydrophobic after a wetting-drying cycle. In a chemically homogeneous film, this behaviour would be difficult to justify. For waterborne acrylic paints, where surfactants and other additives are present, several studies have shown that wet cleaning and immersion can induce surfactant migration, reorganization and partial extraction, together with swelling or whitening of the film in some systems [56–59,63]. In the present case no macroscopic swelling or film disruption was detected, so the observed increase in contact angle is more plausibly linked to a surface re-arrangement with polarity change and roughness increase.

AFM, FTIR and PyGC/MS studies on acrylic emulsions have demonstrated that aqueous cleaning can partially remove or redistribute PEO-based surfactants hydrophilic domains present at the surface, producing measurable changes in gloss, infrared spectra and nano roughness [56,58,60,62]. In related acrylic and vinyl-acrylic latex films, variations in surfactant type and concentration, or covalent incorporation of reactive surfactants, lead to marked differences in water contact angle, confirming the key role of mobile surfactants in controlling water sensitivity [56,57,60]. For vinyl and vinyl-acrylic paints, direct surface studies under wetting-drying cycles remain limited, but compositional work on PVAc and vinyl-acrylic dispersions indicate additive packages analogous to those of acrylic paints, with PEO-type surfactants and PVA dominating the water-soluble fraction [59,61]. Considering literature evidence that water induces the reorganization and partial removal of hydrophilic, surfactant-rich domains, the observed increase in the water contact angle (WCA) could be coherently explained by the depletion of these hydrophilic phases. However, since the presence and concentration of surfactants could not be detected or monitored in this work, further studies are required to fully characterize their presence and rearrangement.

For coated-GNPs layer samples, the presence of GNPs resulted in slightly higher WCA values compared to the coated-control solution ($p < 0.03$), although the absolute difference remained small. Both treatments showed WCA values comparable to those of the commercial silane-siloxane coating (coating, Fig. 8c). This outcome is consistent with the fact that the outermost layer in these systems is the commercial coating, which primarily governs water repellence.

The effect of artificial ageing was also investigated. For untreated paint, rain exposure significantly increased WCA to approximately 120°, and this value was maintained after combined rain and light ageing. Light ageing alone produced a moderate increase, from 70° in unaged samples to about 86° ($p < 0.001$). In contrast, GNPs layer treatment

showed minimal changes after rain or combined ageing, maintaining WCA values near 120°. Light ageing alone caused a slight decrease of about 10° ($p < 0.001$). For coated-GNPs layer treatment, both rain and light ageing induced a small increase in WCA, approximately 10° in each case ($p < 0.01$).

As presented later (*Section 4.2.4. ATR-FTIR*), rain ageing leads to a relevant depletion of calcite from the surface. Mineral fillers like calcite and kaolin are commonly used as extenders in waterborne coatings. Being hydrophilic, these fillers tend to increase the wettability of the resulting surface [53–55]. Therefore, in this case, a plausible explanation for the WCA increase observed after rain exposure on untreated paint is linked to possible surface rearrangement phenomena of both surfactants and mineral-based domains loss.

Overall, these results indicate that the treatment with the dispersant solution alone, strongly influences surface wettability, while the presence of GNPs do not appear to significantly influence the hydrophobicity in the GNPs layer. The coated-GNPs layer systems, dominated by the silane-siloxane coating, show lower WCA than the GNPs layer, even after accelerated ageing.

4.2.3. Roughness evaluation

Surface roughness was evaluated using optical microscopy, and the mean Rq values (Fig. 9) showed clear differences between untreated paint and treatment (both GNPs layer and control), with statistical significance ($p < 0.04$). In general, the treatments led to an increase in Rq compared to unaged paint. This trend aligns with the higher water contact angle (WCA) values observed previously, as surface roughness strongly influences wettability [64,65]. The selective dissolution/removal of mineral fillers and/or surfactants domains can explain the increase in surface roughness. In fact, among the substrate physical properties, surface roughness is a key parameter in defining surface wettability [66–68]. Furthermore, this morphological change is compatible with the proposed surface rearrangement of the paint components induced by the contact with the water-based dispersant solution. This synergistic effect of roughness and surface rearrangement of hydrophilic domains at the surface of paints could promote a more water-repellent condition, as confirmed by the contact angle measurements discussed in *Section 4.2.2*. No significant difference was detected between GNPs layer samples and control treated only with the dispersant solution ($p > 0.05$), indicating that the water system plays a major role in modifying surface morphology, as already observed in WCA measurements. Artificial ageing produced different effects. When light exposure was included, roughness tended to decrease. Conversely, rain ageing alone maintained Rq values comparable to unaged samples ($p > 0.05$) or caused a slight increase, as observed for controls.

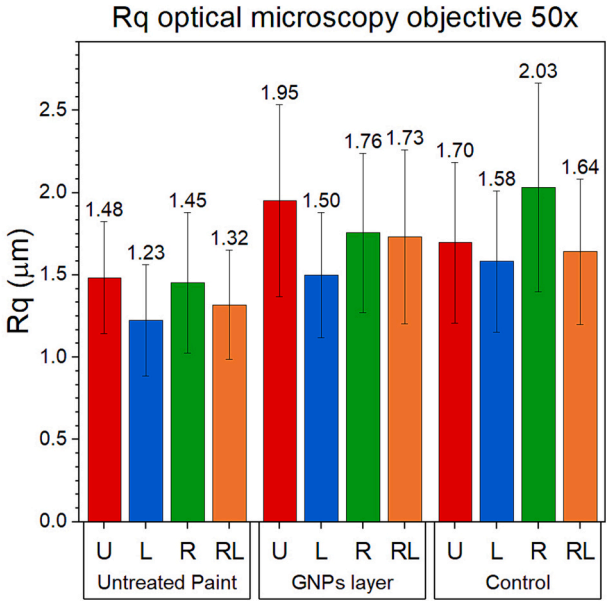

Fig. 9. Mean surface roughness (Rq in µm) for untreated paint, GNPs layer and control, before (unaged U – red) and after artificial ageing (light L – blue, rain R – green, combined rain and light RL – orange). Error bars represent standard deviation. (For interpretation of the references to colour in this figure legend, the reader is referred to the web version of this article.)

In addition to optical microscopy measurements of roughness, an exploratory assessment of surface topography at a different scale was performed using atomic force microscopy (AFM). It is important to underline that, although both techniques aim to describe surface topography, their results are not directly comparable as they operate at completely different scales: optical microscopy provides micrometric profiles over relatively large areas, whereas AFM examines nanometric features within a much smaller area. Despite this fact, the surface roughness inspection at the nanometre length scale can be useful for the interpretation of other data such as contact angle measurements. The AFM profiles are provided in the Supplementary Materials Fig. 2.

AFM profiles confirmed the trend observed at the microscale: GNPs layer and control (dispersant solution without GNPs) exhibited rougher profiles with greater vertical excursions (which are compatible with an increase of Rz value, i.e., the maximum difference between the highest and lowest profile points) than untreated paint. This concordance suggests that the treatment modifies the surface of paint through contact with the water-based dispersion. A more comprehensive study, beyond the scopes of this study, is needed to investigate this phenomenon further, focusing on the surface rearrangement at the nanoscale.

4.2.4. ATR-FTIR

ATR-FTIR characterization allowed to calculate the following ratios between the main paint components: Binder/Calcite (Fig. 10a), Binder/Kaolin (Fig. 10b), and Calcite/Pigment (Fig. 10c). The used characteristic peaks are reported in *Section 3. Methods*. Some informative ATR-FTIR spectra collected from samples are reported in supplementary fig. 3.

Binder/Calcite ratio (Fig. 10a): light ageing caused a decrease in all samples, likely due to the photodegradation of the organic binder. Rain exposure had a strong impact, mainly due to calcite washing out from the paint matrix, as evidenced by the pronounced drop in calcite-related peaks. This effect is particularly evident in all cases when rain is involved (in Fig. 10a and Fig. 10c, R, green, and RL, orange). Moreover, the evaluation of this ratio suggests that the modification caused by the treatment (GNPs layer or control) differs from that caused by rain. In unaged GNPs layer and control, the Binder/Calcite ratio remains essentially unchanged with respect to the untreated paint, indicating that the brief contact with the aqueous dispersions does not induce a significant loss of calcite. This behaviour contrasts with the marked decrease in calcite signals observed after rain ageing, where the ratio clearly reflects calcite washing out from the paint matrix. Taken together with the water contact angle and roughness results, this suggests that the strong increase in hydrophobicity after dipping is more likely associated with the rearrangement and/or partial removal of more labile hydrophilic species, such as surfactants, and with the resulting changes in surface chemistry and micro-topography, rather than with filler depletion. This interpretation is consistent with previous literature observations on acrylic dispersion paints [56–58,60].

Binder/Kaolinite ratio (Fig. 10b): these results confirm the trend observed for the previous evaluated ratio, highlighting the susceptibility of these two fillers to rain exposure.

Calcite/PR112 Pigment ratio (Fig. 10c): in unaged specimens, the application of the treatments (GNPs layer and control) does not significantly modify this ratio relative to the untreated paint ($p = 0.33$), indicating that the short contact with the aqueous dispersions does not alter the balance between calcite and pigment at the surface. After ageing, the ratio is strongly controlled by the type of exposure: light-only

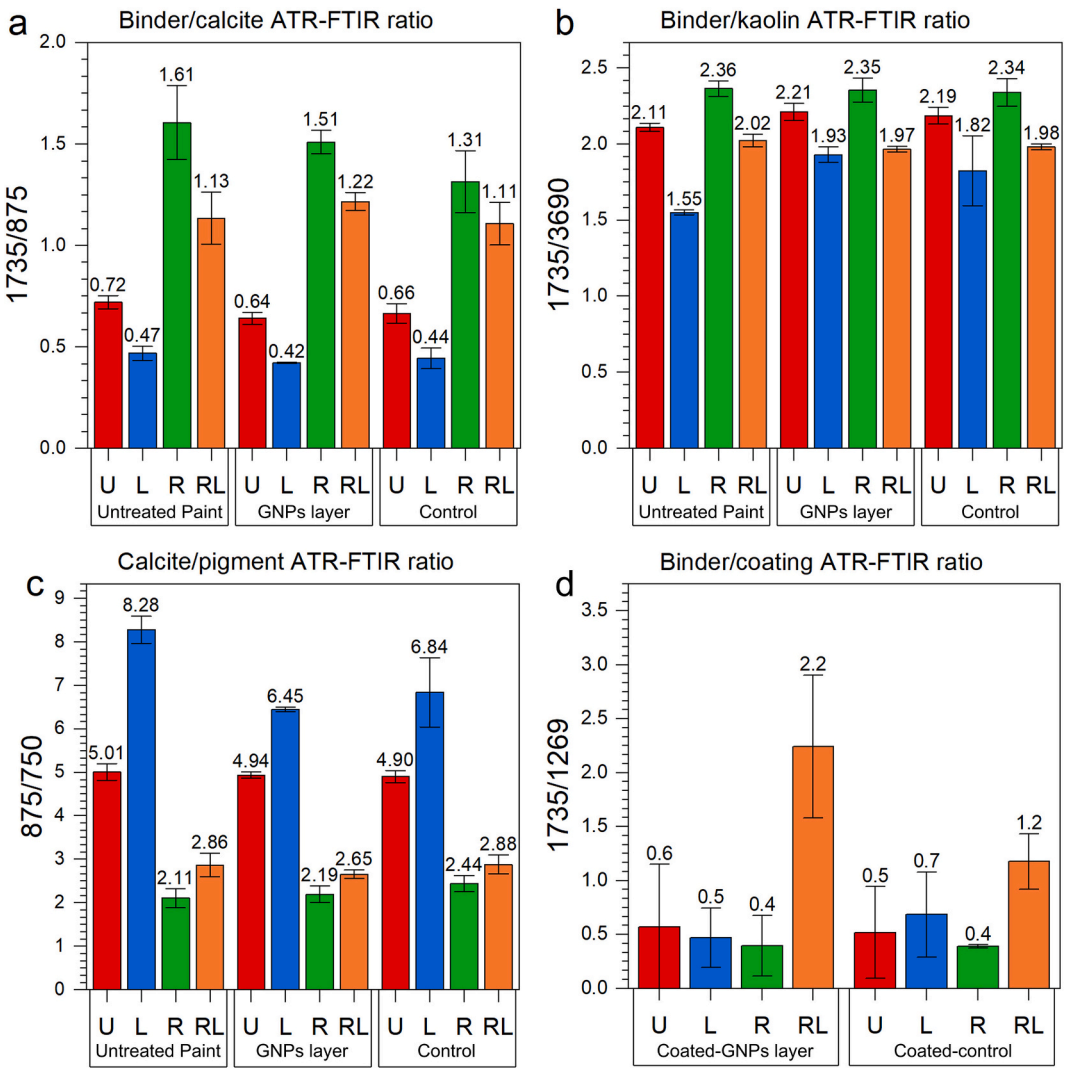

Fig. 10. FTIR peak intensity ratios for (a-c) untreated paint, GNPs layer samples and respective control, and (d) coated-GNPs layer and respective coated-control, under different ageing conditions: U (red) = unaged, L (blue) = light ageing, R (green) = rain ageing, RL (orange) = combined rain and light ageing. For GNPs layer approach the following peak ratios have been evaluated: (a) Binder/Calcite ratio (1735/875 cm^{-1}), (b) Binder/Kaolin ratio (1735/3690 cm^{-1}), (c) Calcite/pigment ratio (875/750 cm^{-1}). (d) FTIR monitoring of coating stability in coated-GNPs layer and respective coated-control. The ratio 1735/1269 (carbonyl group of the paint binder vs. CH_3 bending of Si–CH_3 in the silane-siloxane coating) is shown for coated-GNPs layer and coated-control samples, for different types of ageing. Bars represent mean values and error bars standard deviations. (For interpretation of the references to colour in this figure legend, the reader is referred to the web version of this article.)

ageing (L) leads to an increase in the Calcite/PR112 ratio, consistent with pigment degradation, whereas rain-containing protocols (R and RL) drive the ratio down, reflecting the preferential washout of calcite.

Within rain and combined rain and light ageing, the three sample types follow a broadly similar trend, and no clear statistically significant differences emerge overall among the untreated paint, the GNPs layer and the control. Under light-only ageing, instead, the treatment (GNPs layer and control) shows a significantly smaller increase in the Calcite/PR112 ratio than the untreated paint, indicating that the aqueous dispersant treatment itself favours a better preservation of this balance.

The stability of the coating in coated-GNPs layer and coated-control was evaluated by monitoring the 1735/1269 ratio (Fig. 10d), corresponding to the carbonyl group of the paint binder and the CH_3 bending of the Si–CH_3 bond in the commercial silane-siloxane coating [69]. Under combined rain and light exposure, a marked increase in this ratio was observed, indicating significant instability of the coating and a relative enrichment of the binder component at the surface.

5. Conclusions

This study demonstrated the potential of graphene nanoplatelets (GNPs) as protective surface-applied treatments for outdoor paints, particularly for contemporary muralism. The GNPs layer approach showed excellent aesthetic compatibility, with minimal colour variation after application (ΔE^*_{ab} <3 CIELAB units) across all tested application methods. Consequently, surface-applied GNPs emerged as a cost-effective and minimal intervention strategy, making them highly suitable for the conservation and re-treatment of existing murals.

Surface analyses indicated that the contact of the paint with the water-based dispersion (as observed in control specimens) plays a significant role in altering the hydrophobicity and roughness properties of the painting layers. Furthermore, accelerated ageing tests revealed that this interaction also modified the extent of colour fading. This behaviour can be plausibly linked to the interaction with the polar aqueous environment during the treatment, which may induce surface reorganization phenomena of surfactant and the removal of hydrophilic fillers, such calcite, whose accumulation at the surface is a known driver mechanism

in surface whitening. Notably, chemical stability analysis highlighted that the changes induced by the dipping treatment (whether in GNPs layer or control) are distinct from those caused by rain ageing. Despite the lack of a coating on the GNPs layer, the nanoplatelets demonstrated physical anchoring to the paint substrate, likely due to Van der Waals forces and mechanical interlocking, providing a protective action even after an equivalent of 2 years of accelerated rain ageing. While the limited amount of material used suggests a low risk regarding airborne particles, this remains a preliminary observation; future studies should quantify amount of material applied and its detachment.

GNPs provided additional anti-fading performance, particularly under light exposure alone, where GNPs layer treatment increased the protection factor by more than 12% compared to controls (dispersant only). This protective action is driven by the synergistic mechanisms of attenuation of harmful wavelengths and the physical barrier effect, which hinders the diffusion of oxygen and free radicals. Coated-GNPs layer systems were initially introduced to enhance the stability of GNPs under rain exposure; this strategy proved effective, but it was found to be not strictly necessary, as GNPs showed sufficient adhesion and efficacy even without a coating. Moreover, the observed instability of the silane-siloxane coating under combined rain and light ageing (RL) suggests that the outer coating acts as a sacrificial layer, highlighting that the specific choice of the protective product is crucial for long-term performance.

These results open the way for further research. Future studies should address the quantification and distribution of deposited GNPs, investigate the specific action of dispersant solution systems to the paint formulation, and validate performance through application under real outdoor conditions to better explore long-term performance. Additionally, alternative application strategies should be explored, such as wet-on-wet deposition, where GNPs are applied while the paint or the silane-siloxane coating is still drying, or incorporating them directly into the coating matrix for a single-step application. Overall, applying GNPs via water-based dispersion proved to be an effective strategy for mitigating colour fading in contemporary mural paints, ensuring minimal visual impact and high compatibility with conservation practices.

CRediT authorship contribution statement

Nicolò Guarnieri: Writing – original draft, Visualization, Validation, Methodology, Investigation, Formal analysis, Data curation, Conceptualization. **Sara Goidanich:** Writing – review & editing, Visualization, Validation, Resources, Methodology, Funding acquisition, Conceptualization. **Christos Tsakonas:** Writing – review & editing, Methodology. **George Gorgolis:** Writing – review & editing, Methodology. **Maria Giovanna Pastore Carbone:** Writing – review & editing, Methodology. **George Paterakis:** Writing – review & editing, Methodology. **Gianlorenzo Bussetti:** Writing – review & editing, Visualization, Resources, Investigation, Formal analysis, Data curation. **Costas Galiotis:** Writing – review & editing, Supervision, Resources, Conceptualization. **Lucia Toniolo:** Writing – review & editing, Visualization, Validation, Supervision, Resources, Project administration, Funding acquisition, Conceptualization.

Declaration of competing interest

The authors declare that they have no known competing financial interests or personal relationships that could have appeared to influence the work reported in this paper.

Data availability

Data will be made available on request.

Acknowledgments

The Authors would like to express their deepest gratitude to Prof. Giuseppe Cappelletti (University of Milan, Italy) for kindly providing access to the Water Contact Angle (WCA) equipment for measurements. Special thanks are also due to Irena Todua for her technical assistance during the measurements. The authors also gratefully acknowledge IMCD Italia SpA (Milan, Italy) for providing the product used for the experiments in this study. The authors acknowledge support from the European Research Council (ERC) through the GraphenART (779985) Proof-of-Concept project, and the European Commission for Horizon Europe under the research project GREENART (GA: 101060941). During the preparation of this manuscript, Microsoft Copilot was employed for the purposes of checking the linguistic correctness and flow of the text. The Authors have reviewed and edited the output and take full responsibility for the content of this publication.

Appendix A. Supplementary data

Supplementary data to this article can be found online at https://doi.org/10.1016/j.porgcoat.2026.110148.

References

[1] P. Mezzadri, Contemporary murals in the street and urban art field: critical reflections between preventive conservation and restoration of public art, Heritage 4 (2021), https://doi.org/10.3390/heritage4030142 fasc. 3, Art. fasc. 3, set.
[2] S. Hansen, The role of street art in sustainable development: art and social change, Street Art & Urban Creativity 8 (fasc. 2) (2022) 132–143, dic. 10.25765/sauc.v8i2.616.
[3] L. Pagnin, et al., Protecting street art from outdoor environmental threats: what are the challenges? Coatings 13 (12) (2023) https://doi.org/10.3390/coatings13122044 fasc. 12, Art. fasc. dic.
[4] C. Cianci, et al., Formulation of a new sustainable hybrid coating for the conservation of street-art: Characterization and application, Prog. Org. Coat. 200 (2025), https://doi.org/10.1016/j.porgcoat.2024.109026.
[5] M.R. Caruso, et al., A review on biopolymer-based treatments for consolidation and surface protection of cultural heritage materials, J. Mater. Sci. 58 (fasc. 32) (2023) 12954–12975, ago, https://doi.org/10.1007/s10853-023-08833-5.
[6] E.M. Alonso Villar, et al., Resistance to artificial daylight of paints used in urban artworks. Influence of paint composition and substrate, Prog. Org. Coat. 154 (fasc. 106180) (2021) 106180, mag. https://doi.org/10.1016/j.porgcoat.2021.106180.
[7] J. S. Pozo-Antonio *et al.*, Deterioration of graffiti spray paints applied on granite after a decade of natural environment, Sci. Total Environ., vol. 826, p. 154169, giu. 2022, doi:https://doi.org/10.1016/j.scitotenv.2022.154169.
[8] T. Rivas, et al., Forms and factors of deterioration of urban art murals under humid temperate climate; influence of environment and material properties, Eur. Phys. J. Plus 137 (fasc. 11) (2022) 1257, nov. https://doi.org/10.1140/epjp/s13360-022-03473-1.
[9] D. Cimino, et al., Assessing the (in)stability of urban art paints: from real case studies to laboratory investigations of degradation processes and preservation possibilities, Heritage 5 (fasc. 2) (2022) 581–609, mar. https://doi.org/10.3390/heritage5020033.
[10] J. La Nasa, et al., 60 years of street art: A comparative study of the artists' materials through spectroscopic and mass spectrometric approaches, J. Cult. Herit. 48 (2021) 129–140, mar. https://doi.org/10.1016/j.culher.2020.11.016.
[11] F. Sabatini, et al., Unveiling street art: a multimodal and multitechnique approach for analyzing and mapping painting materials on large murals, Proc. Natl. Acad. Sci. U. S. A. 122 (fasc. 35) (2025), https://doi.org/10.1073/pnas.2504918122 p. e2504918122, set.
[12] N. Guarnieri, et al., VIS-light-induced degradation of street art paints and organic pigments, Appl. Sci. 15 (fasc. 18) (2025) 10188, gen. https://doi.org/10.3390/app151810188.
[13] N. Guarnieri, et al., Rapid chromatic alteration of street art: mechanisms of deterioration of the painting materials of the 20 years of Freedom and Democracy mural, Dyes Pigment. 239 (2025) 112733, ago. https://doi.org/10.1016/j.dyepig.2025.112733.
[14] N. Guarnieri, et al., Preserving the contemporary mural «Musica Popolare» by Orticanoodles in Milan, Italy: deterioration processes and protection performance of commercial coatings, J. Cult. Herit. 75 (2025) 326–332, set. https://doi.org/10.1016/j.culher.2025.08.004.
[15] D. Magrini, et al., A multi-analytical approach for the characterization of wall painting materials on contemporary buildings, Spectrochim. Acta A Mol. Biomol. Spectrosc. 173 (2017) 39–45, feb. https://doi.org/10.1016/j.saa.2016.08.017.
[16] A. Bosi, et al., Street art graffiti: discovering their composition and alteration by FTIR and micro-Raman spectroscopy, Spectrochim. Acta A Mol. Biomol. Spectrosc. 225 (2020) 117474, gen. https://doi.org/10.1016/j.saa.2019.117474.

[17] L. Pagnin, et al., Compatibility and efficacy evaluations of organic protective coatings for contemporary muralism, Coatings 15 (2025), https://doi.org/10.3390/coatings15020166 fasc. 2, Art. fasc. 2, feb.

[18] E. Galvagno, et al., Present status and perspectives of graphene and graphene-related materials in cultural heritage, Adv. Funct. Mater. (2024) 2313043, gen. https://doi.org/10.1002/adfm.202313043.

[19] L. Pagnin, et al., Street art in the rain: evaluating the durability of protective coatings for contemporary muralism through accelerated rain ageing, Coatings 15 (8) (2025) 924, fasc.. ago. https://doi.org/10.3390/coatings15080924.

[20] M. Kotsidi, et al., Graphene nanoplatelets and other 2D-materials as protective means against the fading of coloured inks, dyes and paints, Nanoscale 15 (fasc. 11) (2023) 5414–5428, https://doi.org/10.1039/D2NR05795F.

[21] M. Kotsidi, et al., Preventing colour fading in artworks with graphene veils, Nat. Nanotechnol. 16 (9) (2021), https://doi.org/10.1038/s41565-021-00934-z fasc. 9, Art. fasc.. set.

[22] S. Karimi, et al., A review on graphene's light stabilizing effects for reduced photodegradation of polymers, Crystals 11 (1) (2021), https://doi.org/10.3390/cryst11010003 fasc. 1, Art. fasc.. gen.

[23] Y. Qiu, et al., Antioxidant chemistry of graphene-based materials and its role in oxidation protection technology, Nanoscale 6 (fasc. 20) (2014) 11744–11755, set. https://doi.org/10.1039/C4NR03275F.

[24] P. Pereira, et al., The potential of graphene nanoplatelets in the development of smart and multifunctional ecocomposites, Polymers 12 (fasc. 10) (2020), https://doi.org/10.3390/polym12102189 set.

[25] J. Zhu, et al., Graphene-Enhanced Nanomaterials for Wall Painting Protection, Adv. Funct. Mater. 28, fasc. 44 (2018) 1803872, https://doi.org/10.1002/adfm.201803872.

[26] M.C. Mistretta, et al., Photo-oxidation of polypropylene/graphene nanoplatelets composites, Polym. Degrad. Stab. 160 (2019) 35–43, feb. https://doi.org/10.1016/j.polymdegradstab.2018.12.003.

[27] M. Hasani, et al., Versatile protection of exterior coatings by the aid of graphene oxide nano-sheets; comparison with conventional UV absorbers, Prog. Org. Coat. 116 (2018) 90–101, mar. https://doi.org/10.1016/j.porgcoat.2017.11.020.

[28] N. Nuraje, et al., The addition of graphene to polymer coatings for improved weathering, Int. Sch. Res. Notices 2013 (1) (2013) 514617, https://doi.org/10.1155/2013/514617, fasc.

[29] G.A. El-Hiti, et al., Modifications of polymers through the addition of ultraviolet absorbers to reduce the aging effect of accelerated and natural irradiation, Polymers 14 (fasc. 1) (2021), https://doi.org/10.3390/polym14010020 dic.

[30] M. Kotsidi, et al., Graphene as effective anti-fading agent for the protection of artworks, Invent. Discl. 2 (2022) 100005, gen. https://doi.org/10.1016/j.inv.2022.100005.

[31] D.J. Kim, et al., Degradation protection of color dyes encapsulated by graphene barrier films, Chem. Mater. 31 (fasc. 18) (2019) 7173–7177, set. https://doi.org/10.1021/acs.chemmater.9b01075.

[32] M. Acar, et al., Outdoor performance of wood-plastic composites enhanced with nano graphene-epoxy coating, BioRes 20 (2) (2025) 3075–3084, fasc.. mar. 10.15376/biores.20.2.3075-3084.

[33] P. Cataldi, et al., Graphene nanoplatelets-based advanced materials and recent progress in sustainable applications, Appl. Sci. 8, fasc. 9 (2018), https://doi.org/10.3390/app8091438 ago.

[34] A. Zotti, et al., Polymer nanocomposites based on graphite nanoplatelets and amphiphilic graphene platelets, Compos. Part B Eng. 246 (2022) 110223, nov. https://doi.org/10.1016/j.compositesb.2022.110223.

[35] P. Fu, et al., Modified graphene-FEVE composite coatings: application in the repair of ancient architectural color paintings, Coatings 10 (fasc. 12) (2020), https://doi.org/10.3390/coatings10121162 nov.

[36] L. Toniolo e F. Gherardi, The protection of marble surfaces: the challenge to develop suitable nanostructured treatments, in Advanced Materials for the Conservation of Stone, M. Hosseini e I. Karapanagiotis, A c. di Cham: Springer International Publishing, 2018, pp. 57–78. doi:https://doi.org/10.1007/978-3-319-72260-3_3.

[37] F. Gherardi, et al., Layered nano-TiO2 based treatments for the maintenance of natural stones in historical architecture, Angew. Chem. Int. Ed. 57 (fasc. 25) (2018) 7360–7363, https://doi.org/10.1002/anie.201712752.

[38] H. Lin, et al., Environmental and health impacts of graphene and other two-dimensional materials: A graphene flagship perspective, ACS Nano 18 (8) (2024) 6038–6094, fasc.. feb. https://doi.org/10.1021/acsnano.3c09699.

[39] M. Moreno, et al., Climate Change monitoring with Art-Risk 5: New approach for environmental hazard assessment in Seville and Almería Historic Centres (Spain), Procedia Struct. Integr. 55 (2024) 9–17, https://doi.org/10.1016/j.prostr.2024.02.002.

[40] Art-Risk 5.0 Atlas, gen, https://Artrisk50UsersEarthengineApp/View/Art-Risk5-English, 2025 (consultato gen. 10, 2025).

[41] A. Timoncini, et al., Safeguarding outdoor cultural heritage materials in an ever-changing troposphere: challenges and new guidelines for artificial ageing test, J. Cult. Herit. 59 (2023) 190–201, gen, https://doi.org/10.1016/j.culher.2022.12.003.

[42] UNI EN 15886:2010 - Conservation of Cultural Property—Test Methods—Colour Measurements of Surfaces, 2010.

[43] EN ISO/CIE 11664–4:2019 - Colorimetry — Part 4: CIE 1976 L*a*b* colour space, 2019.

[44] W. S. Mokrzycki e M. Tatol, Colour difference ΔE - a survey, MG&V, vol. 20, fasc. 4, pp. 383–411, apr. 2011.

[45] EN 15802:2009. Conservation of Cultural Property. Test Methods. Determination of Static Contact Angle, 2009.

[46] H. Xue, et al., Study of structural transformation and chemical reactivity of kaolinite-based high ash slime during calcination, Minerals 13 (fasc. 4) (2023) 466, apr. https://doi.org/10.3390/min13040466.

[47] V. Marazioti, et al., Chemical characterisation of artists' spray-paints: a diagnostic tool for urban art conservation, Spectrochim. Acta A Mol. Biomol. Spectrosc. 291 (apr. 2023) 122375, https://doi.org/10.1016/j.saa.2023.122375.

[48] V. Pintus, et al., Accelerated UV ageing studies of acrylic, alkyd, and polyvinyl acetate paints: influence of inorganic pigments, Microchem. J. 124 (2016) 949–961, gen. https://doi.org/10.1016/j.microc.2015.07.009.

[49] E.F. Mooney, The infrared spectra of chlorobenzene and bromobenzene derivatives—III. Toluenes, Spectrochim. Acta 20, fasc. 9 (1964) 1343–1348, set. https://doi.org/10.1016/0371-1951(64)80114-4.

[50] X. Wang, et al., FTIR analysis of the functional group composition of coal tar residue extracts and extractive residues, Appl. Sci. 13 (8) (2023), https://doi.org/10.3390/app13085162 fasc.. Art. fasc. 8, gen.

[51] L. Pagnin, et al., Photodegradation kinetics of alkyd paints: the influence of varying amounts of inorganic pigments on the stability of the synthetic binder, Front. Mater. 7 (2020) 600887, nov. https://doi.org/10.3389/fmats.2020.600887.

[52] A.B. Rodrigues Peruchi, et al., Development of a water-based acrylic paint with resistance to efflorescence and test method to determine the appearance of stains, J. Build. Eng. 35 (2021) 102005, mar. https://doi.org/10.1016/j.jobe.2020.102005.

[53] Y. Ma, et al., Calcium carbonate@silica composite with superhydrophobic properties, Molecules 26 (fasc. 23) (2021) 7180, vol.. nov. https://doi.org/10.3390/molecules26237180.

[54] H. Zhang, et al., Water adsorption on kaolinite basal and edge surfaces, Langmuir 39 (fasc. 22) (2023) 7539–7547, giu. https://doi.org/10.1021/acs.langmuir.2c03282.

[55] H. Xin, et al., Molecular dynamics investigation of mineral surface wettability in oil–water systems: implications for hydrocarbon reservoir development, Minerals 15 (fasc. 11) (2025) 1194, nov. https://doi.org/10.3390/min15111194.

[56] B. Ormsby, et al., Surfactants and acrylic dispersion paints: evaluating changes induced by wet surface cleaning treatments, in: SMITHSONIAN CONTRIBUTIONS TO MUSEUM CONSERVATION - Proceedings from the Cleaning 2010 International Conference. Universidad Politécnica de Valencia and Museum Conservation Institute, Smithsonian Institution Scholarly Press, Washington DC (United States), 2013, pp. 159–164.

[57] S. Digney-Peer, et al., The migration of surfactants in acrylic emulsion paint films, Stud. Conserv. 49 (fasc. sup2) (2004) 202–207, set. https://doi.org/10.1179/sic.2004.49.s2.044.

[58] E. Kampasakali, et al., A preliminary evaluation of the surfaces of acrylic emulsion paint films and the effects of wet-cleaning treatment by Atomic Force Microscopy (AFM), Stud. Conserv. 56 (fasc. 3) (2011) 216–230, set. https://doi.org/10.1179/204705811X13110713013317.

[59] M.F. Silva, et al., Characterization of additives of PVAc and acrylic waterborne dispersions and paints by analytical pyrolysis–GC–MS and pyrolysis–silylation–GC–MS, J. Anal. Appl. Pyrolysis 113 (2015) 606–620, mag. https://doi.org/10.1016/j.jaap.2015.04.011.

[60] H. Zhang, et al., Preparation of PP/2D-nanosheet composites using MoS2/MgCl2- and BN/MgCl2-bisupported Ziegler–Natta catalysts, Catalysts 10 (2020) 596, mag. https://doi.org/10.3390/catal10060596.

[61] M. Novak e B. Ormsby, Poly(Vinyl Acetate) paints: a literature review of material properties, ageing characteristics, and conservation challenges, Polymers, vol. 15, fasc. 22, p. 4348, nov. 2023, doi:https://doi.org/10.3390/polym15224348.

[62] T. Fardi, et al., A novel methodological approach for the assessment of surface cleaning of acrylic emulsion paints, Microchem. J. 141 (2018) 25–39, set. https://doi.org/10.1016/j.microc.2018.04.033.

[63] R. Wolbers, et al., Cleaning of acrylic emulsion paints: preliminary extractive studies with two commercial paint systems, in: SMITHSONIAN CONTRIBUTIONS TO MUSEUM CONSERVATION - Proceedings from the Cleaning 2010 International Conference. Universidad Politécnica de Valencia and Museum Conservation Institute, Smithsonian Institution Scholarly Press, Washington DC (United States), 2013, pp. 147–157.

[64] X. Wang e Q. Zhang, Role of surface roughness in the wettability, surface energy and flotation kinetics of calcite, Powder Technol., vol. 371, pp. 55–63, giu. 2020, doi:https://doi.org/10.1016/j.powtec.2020.05.081.

[65] D. Quéré, Rough ideas on wetting, Phys. A Stat. Mech. Appl. 313, fasc. 1 (2002) 32–46, ott. https://doi.org/10.1016/S0378-4371(02)01033-6.

[66] C. Della Volpe, et al., The combined effect of roughness and heterogeneity on contact angles: the case of polymer coating for stone protection, J. Adhes. Sci. Technol. 14 (fasc. 2) (2000) 273–299, gen. https://doi.org/10.1163/156856100742555.

[67] L. Berti, et al., Contact angle analysis of biocolonized stone surfaces: comparative study of benchtop and portable approaches to advance on-site applications, iScience 28 (fasc. 9) (2025) 113282, set. https://doi.org/10.1016/j.isci.2025.113282.

[68] P. Nguyen-Tri, et al., Recent progress in the preparation, properties and applications of superhydrophobic nano-based coatings and surfaces: a review, Prog. Org. Coat. 132 (2019) 235–256, lug. https://doi.org/10.1016/j.porgcoat.2019.03.042.

[69] O. Cuzman, et al., Natural antibiofouling agents as new control method for phototrophic biofilms dwelling on monumental stone surfaces, Int. J. Conserv. Sci. 2 (2011) mar.